10th International Conference on Short and Medium Span Bridges
Quebec City, Quebec, Canada,
July 31 – August 3, 2018

THICK CONCRETE SLAB BRIDGES: STUDY OF SHEAR STRENGTHENING

Fiset, Mathieu[1,3], Frédéric, Bédard[1], Bastien, Josée[1], Mitchell, Denis[2]
[1] Université Laval, Canada
[2] McGill University, Canada
[3] Mathieu.Fiset.1@ulaval.ca

Abstract: Efficient shear strengthening techniques for thick concrete slabs were studied at Université Laval over the last decade. The strengthening techniques consist of adding drilled-in vertical reinforcing bars and to anchor the bars with bolted plates or expansion anchorage at the bar extremities (i.e. the bars are unbonded to the concrete), or to bond the bars to the concrete with high strength epoxy adhesive (no mechanical anchorage). For concrete members with unbonded bars, experimental loading tests and numerical analysis showed that large diagonal shear cracks are required to activate the shear reinforcement and therefore, the shear behaviour of the members is largely influenced by the stiffness of the strengthening. For specimens with epoxy bonded bars, results showed that the development length of the bars is determined by the locations of the shear cracks and thus, bars may debond before reaching their yielding strength. The efficiency of the shear strengthening techniques is therefore largely influenced by the bars spacing and the stiffness of unbonded shear reinforcement.

1 INTRODUCTION

Thick concrete slab bridges consist of a structural slab deep enough (typically deeper than 500 mm) to resist shear without stirrups. That type of structural system was widely used during the 60s in Canada. These aging bridges may need strengthening due to material degradation and increase of traffic loads. Moreover, the size effect in shear (decrease of concrete shear stress at failure with increasing member depth (Collins and Kuchma 1999, Collins and Mitchell 1991)) was not well understood at the time of the design, but widely affects the shear capacity of thick concrete slabs. The shear capacity determined at the time of the design was therefore overestimated.

After the collapse of the Concorde overpass in Laval in 2010 (Mitchell et al. 2011), shear strengthening methods were investigated for thick concrete slabs that did not contain shear reinforcement. Most of the shear strengthening methods existing in the literature consists of installing reinforcing bars or reinforcing material sheets on the lateral faces of a member (Elstner and Hognestad 1957, Aboutaha and Burns 1994, Nanni et al. 2004, Adhikary and Mutsuyoshi 2006, Teng et al. 2009, Ferreira et al. 2016). Even if these authors demonstrated the efficiency of these methods on beams, their efficiency on large structure like thick concrete slabs is limited. Some authors suggest inserting shear reinforcement into the concrete members (Valerio 2009, Valerio et al. 2011, Mofidi et al. 2016). This approach was studied in this project to strengthen thick concrete slab bridges.

2 REVIEW OF BEAM TESTS

To study the shear strengthening methods, concrete thick slab slices (beam width b_v of 610 mm) similar to the one in Figure 1a were cast and loaded up to shear failure. All methods presented in Figure1b consist

of drilling a hole (about 3 mm larger than de bars diameter) in the concrete (1) at the desired locations of shear reinforcing bars. To properly anchor the bars to the concrete slab strengthened with epoxy bonded bars (denoted as “B”), holes must be cleaned (2) before being filled with epoxy adhesive (3a). Reinforcing bars are inserted and anchored to the concrete (4). Slab specimens P and T are shear strengthened with reinforcing bars unbonded to the concrete. To anchor the lower extremity of the bars, expansion anchorages are used in specimens “T”. The application of a torque opens the shell of the anchorage and anchors the extremity of the bar by friction (3b). The top of the bars in specimens T and the two extremities of the bars in specimens P are anchored with bolted steel plate (5). While most of the specimens were shear strengthened, some specimens without shear reinforcement as well as specimens containing conventional stirrups (denoted as “S”) were tested to determine reference shear capacities. These methods are effective on large elements such as thick concrete slabs. The installation is rapid and easy, and the added bars can be installed from the top or the bottom of a slab.

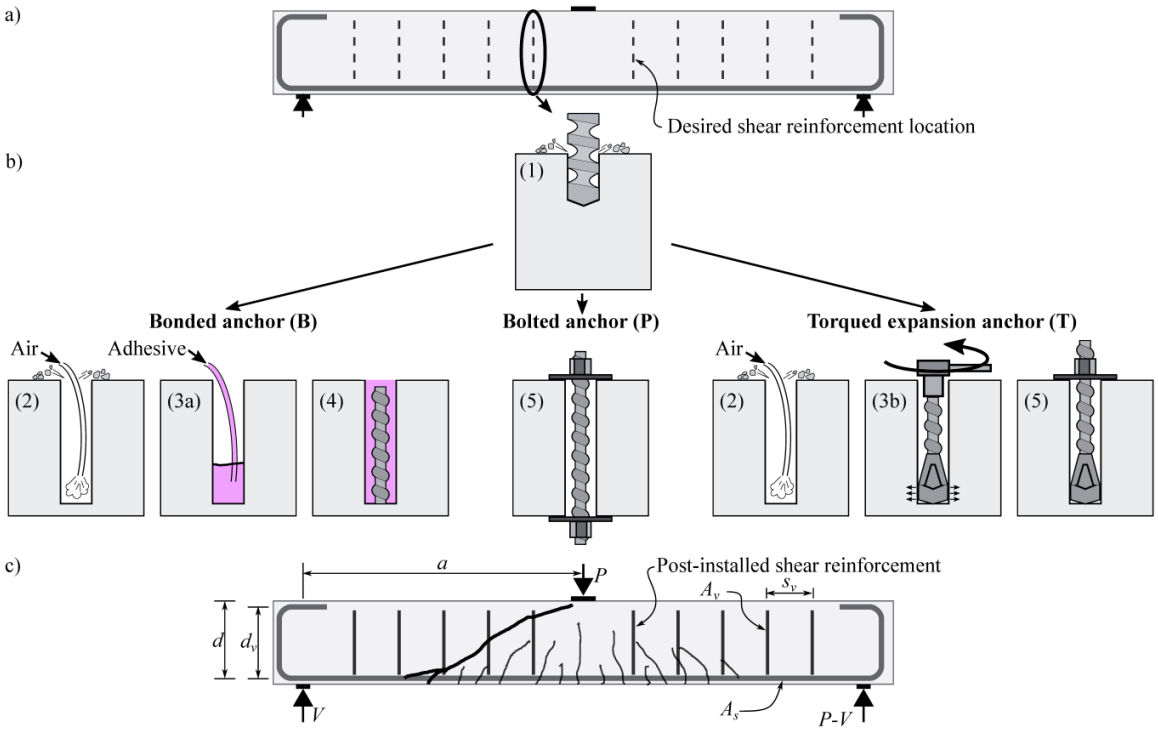

Figure 1: a) Initial unstrengthened thick slab, b) installation of post-installed shear reinforcement and c) loading of the shear strengthened specimens

Two specimens of each type were tested, for a total of 22 shear tests. For all specimens, the shear depth d_v was higher than 300 mm (d_v = 0.9d) hence, size effect in shear can be experienced (Bentz 2005). To obtain a shear failure, a bending reinforcement ratio $A_s/(b_v d)$ larger than 1.17% (Table 1) was selected as well as a shear span to depth ratio a/d between 2.8 and 3.6 (Figure 1c). Except for specimens P1, the transverse reinforcement spacing ratio s_v/d_v was between 0.61 and the maximum of 0.75 permitted by CSA-S6 (2014). A concrete compressive strength f_c' of about 35 MPa and maximum aggregate size a_g of 19 mm were selected to represent design of existing thick concrete slabs bridges in the 60’s. The yielding strength of the transverse reinforcement f_y varies between 448 and 642 MPa so that all specimens indicated as #1 contain a similar transverse reinforcement strength ratio $\rho_v f_y = A_v f_y/(b_v s_v)$ between 0.77 and 1.09 MPa. Also, $\rho_v f_y$ is larger than the minimum amount of $0.06\sqrt{f_c'}$ = 0.35 MPa required by CSA-S6. According to the manufacturer, the properties of the adhesive are as follows: compressive strength of 42.7 MPa, tensile strength of 43.5 MPa and compressive modulus of 1493 MPa (Hilti 2005). More details about the tested specimens are given by Provencher (2010), Cusson (2012), Fiset et al. (2017).

Table 1: Summary of member properties and experimental tests

#	Anchor type	f_y (MPa)	$A_s / b_v d$ (%)	d_v (mm)	s_v / d_v	$\rho_v f_y$ (MPa)	V_R (kN)	V_n (kN)	V_R / V_n	V_u (kN)	V_R-V_u / $b_v d_v$ (MPa)
S1	Stirrups	448	1.65	625	0.61	0.77	768	804	0.96	*449	0.84
T1	Expan.	642	1.65	625	0.61	0.81	585	810	0.72	*449	0.36
P1	Plate	517	1.65	625	1.60	1.09	843	920	0.92	*449	1.03
B1	Bonded	448	1.65	625	0.61	0.77	756	809	0.93	*449	0.81
B2	Bonded**	448	1.65	625	0.61	1.55	882	1083	0.81	*449	1.14
B3	Bonded	480	1.17	629	0.75	0.67	498	705	0.71	384	0.30
B4	Bonded	436	2.05	359	0.72	0.55	302	428	0.71	288	0.06
B5	Bonded	480	3.10	333	0.72	1.31	471	602	0.78	324	0.72

*Shear carried by concrete at the propagation of the critical diagonal crack in member P1

** Bonded bars were inserted from both the top and the bottom of these members and overlapped at mid-depth over 300 mm. The distance between the bottom of one bar and the top of the other bar is 710 mm.

3 BEAM RESPONSES

The average shear capacity of the strengthened specimens V_R is presented in Table 1 and compared to the predicted nominal capacity V_n, which is determined as following according to the Canadian standard CSA-S6 for elements respecting the minimum amount of transverse reinforcement.

[1] $V_n = V_c + V_s = 2.5\beta\phi_c f_{cr} b_v d_v + \phi_s \rho_v f_y \cot\theta b_v d_v$

Where $\phi_c = \phi_s = 1$ for the nominal capacities, β is a factor accounting for the concrete contribution resisting shear and takes into account the size effect in shear, the concrete cracking strength $f_{cr} = 0.4 f_c'^{0.5}$ and θ is the orientation of the principal compressive stress. For the strengthened specimens, β varies between 0.14 and 0.19 and θ varies between 34° and 37°. Note that a very similar approach is specified by AASHTO (2014), CSA-A23.3 (2014) and the fib model code (2013). The Canadian standard results in a very good prediction of the shear capacity of members with stirrups "S" ($V_R/V_n = 0.96$). As expected, it overestimates the capacity of all members with post-installed shear reinforcement. For the specimens with bonded bars "B", it can be seen that increasing the ratio of s_v/d_v increases the shear capacity overestimation. For example, the shear capacity of the specimens B1 with a spacing ratio of 0.61 is overestimated by 7% ($V_R/V_n = 0.93$), while it is overestimated by 29% ($V_R/V_n = 0.71$) for specimens B3 having a spacing ratio of 0.75. By comparing the shear capacity of the reference specimens without shear reinforcement V_u to the shear strengthened specimens capacity V_R, it can be seen that all strengthening methods increase the shear capacity. However, that increase widely varies from one specimen to another. To compare the increase in shear stress according to the transverse reinforcement strength ratio $\rho_v f_y$, the efficiency of shear strengthening E_v (Equation [2]) is compared in Figure 2a.

[2] $E_v = \dfrac{V_R - V_u}{\rho_v f_y b_v d_v}$

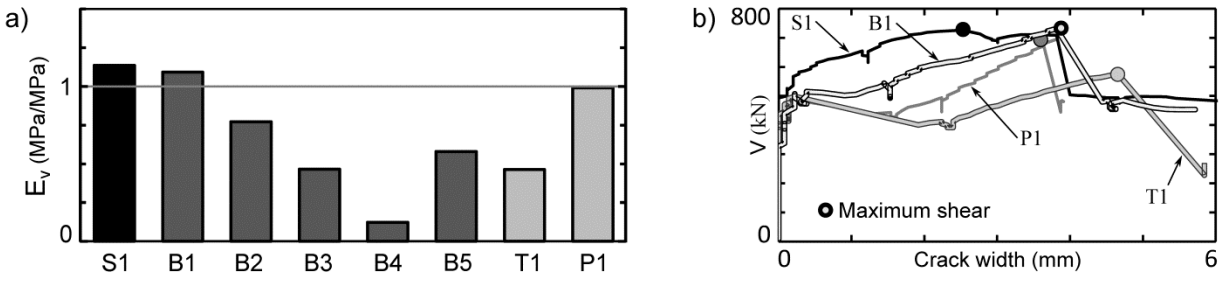

Figure 2: a) Efficiency ratio E_v of shear strengthening and b) shear versus critical diagonal crack width

It can be observed in Figure 2a that the efficiency of shear strengthening in specimens B1 and P1 (E_v = 1.04 and 0.95 respectively) is similar to the specimens S1 with stirrups (E_v = 1.08). Indeed, both the specimens P1 and B1 experienced the largest increase of shear strength $(V_R-V_u)/(b_v d_v)$ of 1.03 and 0.81 MPa, respectively. Increasing the spacing ratio to about 0.75 (B3, B4 and B5) significantly reduces E_v. The efficiency ratios E_v were 0.41 and 0.51 for specimens B3 and B5, respectively. The specimens B4 experienced almost no increase of shear strength and the ratio E_v of 0.11 was the lowest of all tested specimens. The specimens B2, with twice the amount of shear reinforcement, experienced the largest increase of shear capacity, but the efficiency of shear strengthening is lower than the specimens B1. Factors described in the following sections can explain the efficiency of shear strengthening.

4 FACTORS AFFECTING SHEAR STRENGTHENING EFFICIENCY

4.1 Effect of the critical crack width

Figure 2b presents the shear versus the critical crack width of the shear strengthened specimens #1. It can be observed that specimens P1 and T1 with unbonded shear reinforcement present a decrease of shear after diagonal cracking. At that moment, the diagonal crack width rapidly increases from about 0 to 1.6 mm and 2.4 mm for P1 and T1, respectively. For unbonded bars, the load is only transferred from the concrete to the bars at their extremities. The bar strain being ΔL/L, a large elongation ΔL is required to increase the strain along the length L, length corresponding to the total unbonded bar length. Since ΔL corresponds to the displacement between the bar end anchorages, it is related to the crack width and the stiffness of the anchoring system (Fiset et al. 2016). A large crack is therefore required to activate an unbonded bar. For comparison, the load can be transferred to the concrete by bond along a shorter distance for specimens S1 and B1, thereby reducing the length L and the required crack width to activate the bars. Thus, specimens B1 experienced a small decrease of shear at shear cracking and specimens S1 experience no decrease of shear up to the maximum shear. At the maximum shear, specimens S1 and B1 contained a large number of diagonal cracks and the width of critical diagonal crack was 2.5 and 3.8 mm, respectively. For comparison, the specimens with unbonded bars, P1 and T1, exhibited one large diagonal crack of 3.6 and 4.7 mm, respectively. According to Collins and Mitchell, the shear carried by aggregate interlock $V_{c,agg}$ at diagonal crack being a function of the crack width "w" (Equation [3], where $k_{ag} = 24/(16+a_g)$) the larger crack at shear failure leads to a lower aggregate interlock. Therefore, a smaller increase of shear capacity and a lower shear reinforcement efficiency ratio E_v are observed for specimens P1, T1 and B1 than the reference specimens S1. The shear strengthening efficiency is therefore related to the crack width and thus, the aggregate interlock shear capacity at member failure. Also, the angle θ (refer to Equation [1]) is related to the yielding of transverse reinforcement (Rahal and Collins 1999). Thus, it is expected that the large crack required to activate unbonded bars may affect θ.

$$[3]\quad V_{c,agg} = \frac{0.18\sqrt{f'_c}}{0.31 + k_{ag} w} b_v d_v$$

4.2 Effect of bonded bars behaviour

For bonded shear reinforcement, the shear carried by shear reinforcement has to be transferred to the concrete by bond hence, the shear strengthening efficiency depends on the bond strength f_b. Villemure et al. (2016) carried out confined pull-out tests to determine the local bond stress versus slip relationship of the epoxy bonded bars used in specimens B. Figure 3a presents the experimental relationship as well as a general model curve (Lowes et al. 2004). This curve is curvilinear up to the maximum bond stress f_{b0} and shows a plateau starting at a slip of about 0.8 to 1 mm. That stress plateau ends at a slip of about 2 mm and the bond stress decreases to about $0.4f_{b0}$ at slip of 10 mm for the bar diameter used. For the epoxy bonded bars used in specimens B, the maximum bond capacity of the epoxy adhesive f_{b0} was estimated as 32.5 MPa. However, Eligehausen et al. (2006) suggested limiting the bond strength to the concrete breakout capacity with Equation [4].

$$[4]\quad f_b = K\sqrt{f'_c \ell}/d_b \le f_{b0}$$

Where K equals 4.7 for epoxy bonded bars, ℓ is the bar embedded length and d_b is the bar diameter (d_b = 16 mm for B1, B2, B3 and B5, and d_b = 11 mm for B4). Typically, the bond strength f_{b0} is higher than f_b determined with Equation [4]. However, the bond versus slip relationship can be used in FE analysis and to estimate the crack width (Fernández Ruiz et al. 2007, Fiset et al. 2014). Limiting the bar axial stress to the bar yielding strength, the maximum bar axial stress f_{smax} can be determined from the bond strength in Equation [4] with Equation [5].

[5] $f_{smax} = 4f_b\ell/d_b \leq f_y$

Figure 3b presents a section of a shear strengthened thick slab with bonded bars. Before shear failure, the member contains a large number of diagonal cracks equally spaced, but randomly located. The embedded length of the bars defined by the diagonal cracks varies in the member as well as the bond strength f_b and f_{smax} (Figure 3c). From Equations [4] and [5], the bond strength at the bonded bar yielding f_{by} and the bar development length ℓ_d can be determined as following.

[6] $f_{by} = (K/2)^{2/3}\left(f_c' f_y / d_b\right)^{1/3} \leq f_{b0}$

[7] $\ell_d = \dfrac{f_y d_b}{4 f_{by}}$

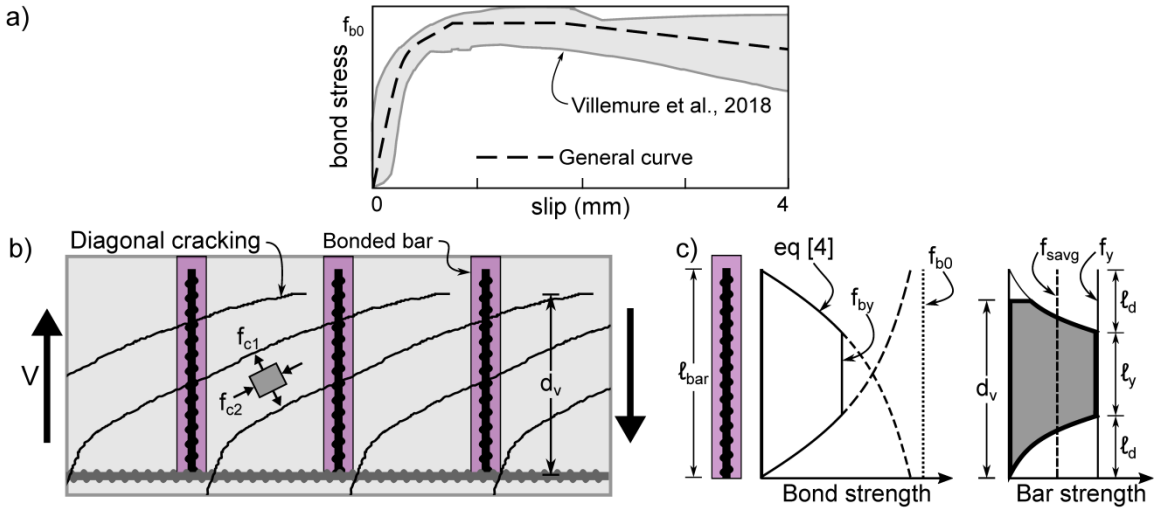

Figure 3: a) Adopted bond behaviour, b) bonded bars in a beam and c) development of a bonded bar

5 EFFECT OF DIAGONAL CRACK ORIENTATION AND DIAGONAL COMPRESSION ON BONDED BARS

In the member illustrated in Figure 3b, shear is carried between cracks by diagonal tension f_{c1} and compression f_{c2} in the concrete. Before shear failure of typical concrete members ($\theta \approx 35°$), f_{c1} is small and f_{c2} is about $2V/(b_v d_v)$ so that shear between cracks is mainly carried by diagonal compression. That diagonal compression may confine the anchorage and results in improved bond strength and concrete capacity. However, the inclination of the crack surface may also reduce the concrete area resisting pull-out and thus, reduces the concrete breakout capacity. To investigate this effect, finite element (FE) modelling of inclined pull-out representing beam conditions was analyzed in the numerical tool VecTor3. That software includes several material and element options adapted to reinforced concrete structures, such as predefined concrete and steel behaviour as well as bond elements for the modelling of reinforcing bars to concrete interfacial behaviour. For more details about modelling, bonded bars and VecTor, refer to Fiset et al. and ElMohandes et al. (2013).

The section of a member resisting shear is presented in Figure 4a and compared to the FE model of inclined pull-out in Figure 4b. In order to represent the stress conditions in a member resisting shear, the displacement "u" is restrained in "x" and "y" directions at the top of the crack hence, the load applied to the bar has to be transferred to the concrete by compression. Taking advantage of the symmetry plane (uz = 0), half of the width of the pulled-out specimen is modelled. Embedded length of the analyzed bonded bars was 50 mm or 80 mm thus, the bar yielding strength is higher than the concrete breakout capacity (Equation [5]). To avoid any effect of concrete cover and bonded anchorage, the model is 1000 mm width (in "z" direction), at least 1000 mm height (in "y" direction) and at least 1000 mm long (in "x" direction). The size of the model in "x" and "y" directions are adjusted to the desired angle, but respects a minimum distance of 200 mm above the anchorage and the number of elements in the anchorage region. In that region, the element size in "y" and "z" directions is no longer than 10 mm. To model the drilled hole filled with epoxy adhesive, elements located at a distance of 0.6 d_b around the bar were modelled with the mechanical properties of the epoxy adhesive. For comparison, one model was analyzed without the adhesive elements to represent a cast-in-place reinforcing bar. A combination of the following parameters was analyzed: d_b of 16 mm and 25 mm and f_c' of 35 MPa and 60 MPa. The concrete tensile strength is taken as $0.33\sqrt{f_c'}$ and the other concrete properties were defined by the default values in VecTor (refer to Fiset at al). The inclination of the analyzed cracking plane ranges between 20° and 70° and one typical pull-out (θ = 0°) was modelled and compared to Equation [4] for model validation.

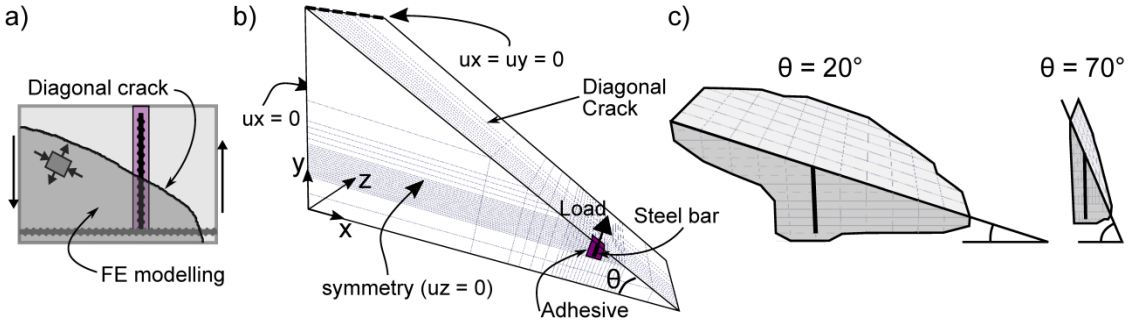

Figure 4: a) Location of the model in a shear strengthened specimen, b) FE modelling of a bonded bar at an inclined crack and c) FE prediction of the failure surface for θ = 25° and θ = 70°.

For all analyzed specimens, a pull-out failure occurred before yielding of the bar, as expected. Figure 5a presents the ratio between the resistance "R" determined from FE analysis and the predicted one by Equation [5] for a conventional pull-out (θ = 0°). Figure 5b presents the ratio between the resistance R determined by FE analysis for inclined pull-out to a typical pull-out (θ = 0°). It can be seen in Figure 5a (θ = 0°) that the FE model predicts similar pull-out capacity than the design Equation [5] for both epoxy bonded and cast-in-place reinforcing bars. On average, R_{FE}/R_{calc} is equal to 0.98 (covariance of 4.5%), which confirms the validity of FE analysis. The largest difference was observed for the specimen with f_c' = 60 MPa. For that specimen, the FE model underestimates the capacity by 7% (R_{FE}/R_{calc} = 0.93). To avoid overestimation of the ratio between R_θ and $R_{0°}$ in Figure 5b, the reference capacity of a flat pull-out $R_{0°}$ was determined from the FE analysis, except for specimens with f_c' = 60 MPa for which $R_{0°}$ is taken from Equation [5]. It can be observed in Figure 5b that the variation of the resistance is very small up to an inclination θ of 25°. For the specimen with f_c' = 60 MPa, R_θ at 20° is very similar to $R_{0°}$ determined with Equation [5] and higher than the FE capacity at 0°. For θ between 25 and 40 °, some models experienced increase of the anchorage capacity (up to 7% at θ = 30°) due to concrete confinement, while others showed reduction of their capacity (up to 20% at θ = 40°). For θ larger than 40°, all specimens showed reduction of their capacity, up to 52% at θ = 70°. That reduction can be explained by the reduction of the concrete cone surface resisting the pull-out as illustrated in Figure 4c. Typically, large failure surface can be observed for models with θ < 35°, while increasing θ over 40° rapidly reduces the concrete cover for the failure surface illustrated in Figure 4c for θ = 70°. According to FE analysis, that effect can be captured by Equation [8] illustrated in Figure 5b, where Ω_θ corresponds to the ratio R_θ / $R_{0°}$.

[8] $\Omega_\theta = 0.30 + \tanh\left(\frac{10}{\theta - 25}\right) \leq 1$ [deg]

From Equation [8] and FE results, the pull-out capacity of bonded shear reinforcement installed in typical concrete members with θ ≤ 36° are not affected by the orientation of the diagonal crack ($\Omega_\theta = 1$). When θ > 36°, reduction of the anchor capacity is expected and Equation [8] can be used to multiply the factor K in Equations [4] and [6] to estimate the bonded shear reinforcement capacity.

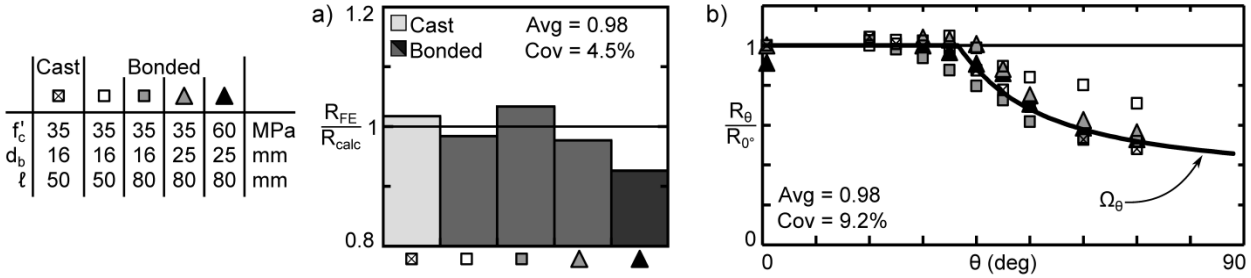

Figure 5: a) Ratio between FE and standard predicted capacity with Equation [5] (θ = 0°), and b) effect of the crack orientation on FE predicted anchorage pull-out capacity.

6 DESIGN RECOMMENDATIONS FOR BONDED SHEAR REINFORCEMENT

For the tested specimens, the development lengths ℓ_d determined with Equation [7] were 102 mm for B1, 104 mm for B2, 108 mm for B3 and B5, and 63 mm for B4. Figure 6 compares the cracking pattern of specimens B1 and B3. In this figure, the critical diagonal crack is illustrated in bold, while the other thin grey lines represent the other cracks. The location where the critical diagonal crack intercepts shear reinforcement and the associated embedded length are indicated with arrows. For the illustrated specimen B1, the critical crack is intercepted by three shear reinforcing bars, while two are intercepted near their extremities for the specimen B3. Therefore, two shear reinforcing bars are fully developed in specimen B1 ($\ell > \ell_d$), while one is intercepted at about 30 mm from its lower extremity and hence is partially developed. For the specimen B3, one of the bars embedded length is about 57 mm on average hence, only one shear reinforcing bar is fully developed. The efficiency of a bar η representing the average bar capacity f_{savg} can be determined such that $\eta f_y = f_{savg}$ from the shaded area in Figure 3c. From Equation [5] to [7], η can be determined with Equation [9].

[9] $\eta = \left(\ell_{bar} - 1.2\ell_d\right)/d_v \leq 1$

That ratio considers that the bar slip is large enough to develop the bond strength, but small enough so that deboning has not occurred yet, i.e. the bar slip is between 0.8 and 2 mm according to the tests carried out by Villemure et al. (refer to Figure 3a). For specimens B1 and B3, η = 0.86 and 0.82 respectively, and drops to 0.75 and 0.64 for specimens B4 and B5, respectively. It therefore appears that the efficiency of the shear strengthening in Figure 2a is related to η.

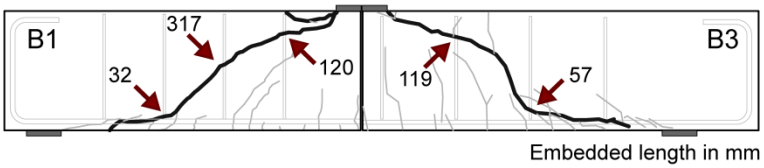

Figure 6: Diagonal cracking and average embedded length of specimens B1 and B3

6.1 Evaluation of maximum shear capacity

It is recommended to include the bar efficiency factor η in the design of members with epoxy bonded bars to determine their shear capacity, their minimum amount and their maximum transverse spacing. Considering the average strength of bonded shear reinforcement, their contribution to the shear capacity V_{sB} can be determined with Equation [10].

[10] $V_{sB} = \phi_s \eta \rho_v f_y \cot\theta b_v d_v$

The minimum amount of shear reinforcement has to be provided to prevent sudden shear failure at the formation of the first diagonal cracking (Yoon et al. 1996). Thus, the shear capacity provided by transverse reinforcement has to be higher than the concrete shear capacity at first diagonal cracking. According to CSA-S6, the minimum ratio of conventional stirrups $\rho_v f_y$ is $0.06 f_c'^{0.5}$. Considering the average strength of bonded shear reinforcement, the minimum bonded shear reinforcement strength ratio has to be designed with Equation [11].

[11] $\eta \rho_v f_y \geq 0.06\sqrt{f_c'}$

Fiset et al. also proposed to include the efficiency ratio of bonded shear reinforcement to reduce the maximum spacing of transverse bonded shear reinforcement. The maximum spacing of transverse reinforcement is defined so that every diagonal crack at a predefined angle is able to develop at least the yielding strength of two consecutive shear reinforcing bars. Considering the average capacity, the maximum spacing of bonded shear reinforcement can be determined with Equation [12], where k_v is the maximum spacing ratio for a member with stirrups where k_v = 0.75 for CSA-S6 and k_v = 0.80 for AASHTO.

[12] $s_v / d_v \leq \eta k_v$

It can be expected that members having a transverse reinforcing bars spacing ratio between ηk_v and k_v experience a partial development of transverse reinforcement and larger diagonal cracks. Table 2 presents the revised capacities, amount of shear reinforcement and maximum spacing according to these recommendations. Comparing the ratio of the experimental shear capacity V_R to the predicted capacity with and without the suggested efficiency factor η (V_{nB} and V_n, respectively), it can be seen that the coefficient η significantly improves the accuracy of the shear capacity prediction. Indeed, the average ratio V_R/V_n increases by 11% (from 0.79 to 0.90) when η is used. For all members respecting both the maximum spacing ratio ηk_v and the minimum amount of shear reinforcement, the shear capacity predictions are very good (V_R/V_{nB} = 1.00 and 1.02 for specimens B1 and B2, respectively). For specimens B4, the spacing of bonded shear reinforcement does not respect the spacing for bonded bars ηk_v of 0.56 (for CSA-S6). Moreover, specimens B4 contains a transverse reinforcement strength ratio $\eta \rho_v f_y$ of 0.41 MPa, which is very close to the minimum permitted of 0.35 MPa. This may explain why specimens B4 have the smallest shear strengthening efficiency E_v of 0.11 (Figure 2).

Table 2: Predicted capacity of specimens with bonded shear reinforcement

#	θ (deg)	Ω_θ	η	$\eta\rho_v f_y$ (MPa)	s_v / d_v	Maximum spacing ηk_v (CSA-S6)	Maximum spacing ηk_v (AASHTO)	V_{sB} (kN)	V_{nB} (kN)	V_R/V_n	V_R/V_{nB}
B1	34.9	1.00	0.86	0.66	0.61	0.64	0.69	363	759	0.93	1.00
B2	35.6	1.00	0.61	0.94	0.61	0.70*	0.75*	499	859	0.81	1.02
B3	36.0	1.00	0.82	0.55	0.75	0.62	0.66	290	655	0.71	0.76
B4	33.8	1.00	0.75	0.41	0.72	0.56	0.60	135	389	0.71	0.77
B5	33.6	1.00	0.64	0.84	0.72	0.48	0.51	257	490	0.78	0.96
									Avg	0.79	0.90
									Cov	11.5%	14.0%

*The maximum spacing of specimens B2 has to be determined with η = (710-1.2×104)/625 = 0.94 due to the bonded bar overlapping

7 CONCLUSIONS

For all shear strengthened members, it could be concluded that shear strengthening improves shear and deformation capacity compared to concrete thick slabs without shear reinforcement. The following specific conclusions also resulted from the analysis of beams with mechanically anchored but unbonded shear reinforcement:

- At shear cracking, members with unbonded bars experienced a large decrease of shear and rapid propagation of a large diagonal crack;
- A large diagonal shear crack is required to activate the shear reinforcement, thereby reducing concrete aggregate interlock shear capacity;
- The efficiency of shear strengthening with unbonded bars depends on the shear strengthening system stiffness and the crack width;

For members with unbonded shear reinforcement, future design methods will have to consider these larger cracks, resulting in lower aggregate interlock shear capacity factor β, and the unbonded bar stiffness, which can influence the design angle θ (Rahal and Collins).

The following conclusions resulted from the analysis of beams with epoxy bonded shear reinforcement:

- The location of diagonal shear cracks determines the bonded bars embedded length. Bars with short embedment failed by debonding before their yielding strength while longer embedded bars yielded at member failure;
- The maximum transverse reinforcement spacing of 0.75 d_v prescribed by the Canadian Highway Bridge Design Code CSA-S6 for stirrup leads to a large shear capacity overestimation;
- Good prediction of the shear capacity was achieved by the current design methods for the tested members with bonded reinforcement having a spacing ratio of 0.61d_v;

The effects of anchorage of the bonded bars were also studied with experimental pull-out tests and FE analysis. Design criteria were suggested to determine the shear capacity of members with bonded shear reinforcement. It appears that the capacity of tested members respecting the minimum amount and the maximum spacing of bonded shear reinforcement is very well predicted. Tested members respecting the minimum amount of bonded shear reinforcement but having a maximum spacing between the one specified for stirrups and the one for bonded bars experienced a smaller increase of their shear capacity and the proposed design method overestimates the shear capacity. More research is required to better understand the behavior of drilled-in bonded bars used for shear strengthening. Future research will analyze this type of member as well as propose a design method for members with unbonded shear reinforcement.

Acknowledgements

This research was made possible by the funding from the Natural Sciences and Engineering Research Council of Canada (NSERC) and the “Fonds de Recherche du Québec – Nature et Technologies” (FRQNT). The authors also wish to acknowledge the work of Philippe Provencher, Benoit Cusson and Felix-Antoine Villemure who performed the experimental slab tests and the pull-out tests.

References

AASHTO. 2014. *LRFD Bridge Design Specifications 7th Ed. .* American Association of State Highway and Transportation Officials, Washington US.

Aboutaha, R. S., and Burns, N. H. 1994. Strengthening of Prestressed Concrete Composite Beams Using External Prestressed Stirrups. *PCI Journal*: **39**(4), 64-74.

Adhikary, B. B., and Mutsuyoshi, H. 2006. Shear Strengthening of Reinforced Concrete Beams Using Various Techniques. *Construction and Building Materials*: **20**(6), 366-373.

Bentz, E. C. 2005. Empirical Modeling of Reinforced Concrete Shear Strength Size Effect for Members without Stirrups. *ACI Structural Journal*: **102**(2), 232-241.

Collins, M. P., and Kuchma, D. 1999. How Safe Are Our Large, Lightly Reinforced Concrete Beams, Slabs, and Footings? *ACI Structural Journal*: **96**(4), 482-490.

Collins, M. P., and Mitchell, D. 1991. *Prestressed Concrete Structures.* Prcnticc-Hall, Englewood Cliffs, New Jersey, USA.

CSA-A23.3. 2014. Design of Concrete Structures. Mississauga, Ont.: Canadian Standards Association

CSA-S6. 2014. *Canadian Highway Bridge Design Code and Commentary.* Canadian Standards Association, Mississauga, ON, Canada.

Cusson, B. 2012. *Renforcement des dalles épaisses en cisaillement.* (M.Sc. Thesis) Université Laval, Québec, Canada.

Eligehausen, R., Cook, R., and Jorg, A. 2006. Behavior and Design of Adhesive Bonded Anchors. *ACI Structural Journal*: **103**(6), 822-831.

ElMohandes, F., Vecchio, F. J., and Trommels, H. 2013. *Vector3.* University of Toronto, Toronto, Canada.

Elstner, R. C., and Hognestad, E. 1957. Laboratory Investigation of Rigid Frame Failure. *ACI Journals*: **28**(7), 637-668.

Fernández Ruiz, M., Muttoni, A., and Gambarova, P. G. 2007. Analytical Modeling of the Pre- and Postyield Behavior of Bond in Reinforced Concrete. *Journal of Structural Engineering*: **133**(10), 1364-1372.

Ferreira, D., Bairán, J. M., and Marí, A. 2016. Shear Strengthening of Reinforced Concrete Beams by Means of Vertical Prestressed Reinforcement. *Structure and Infrastructure Engineering*: **12**(3), 394-410.

fib. 2013. *fib Model Code for Concrete Structures 2010.* Ernst and Sohn, Lausanne, Switzerland.

Fiset, M., Bastien, J., and Mitchell, D. 2014. Drilled-in Shear Reinforcement for Concrete Thick Slabs: Modelling Aspects. *The 10th fib International PhD Symposium in Civil Engineering*, Université Laval, Québec, Canada, 1: 481-486.

Fiset, M., Bastien, J., and Mitchell, D. 2017. Methods for Shear Strengthening of Thick Concrete Slabs. *Journal of Performance of Constructed Facilities*: **31**(3), 10.

Fiset, M., Parenteau, A., Bilodeau, S., Bastien, J., and Mitchell, D. 2016. Behaviour of thick concrete members with unbonded transverse reinforcement. *Proceedings of 11th fib International PhD Symposium in Civil Engineering*, fib, Tokyo, Japan, 385-392.

Hilti. 2005. Hilti Fastening Technology Manual B 2.11. Schaan, Liechtenstein.

Lowes, L. N., Moehle, J. P., and Govindjee, S. 2004. Concrete-Steel Bond Model for Use in Finite Element Modeling of Reinforced Concrete Structures. *ACI Structural Journal*: **101**(4), 501-511.

Mitchell, D., Marchand, J., Croteau, P., and Cook, W. D. 2011. Concorde Overpass Collapse: Structural Aspects. *Journal of Performance of Constructed Facilities*: **25**(6), 545-553.

Mofidi, A., Chaallal, O., Cheng, L., and Shao, Y. 2016. Investigation of Near Surface Mounted Method for Shear Rehabilitation of Reinforced Concrete Beams Using Fiber Reinforced Polymer Composites. *Journal of Composites for Construction*: **20**(2), 14.

Nanni, A., Di-Ludovico, M., and Parretti, R. 2004. Shear Strengthening of a PC Bridge Girder with NSM CFRP Rectangular Bars. *Advances in Structural Engineering*: **7**(4), 97-109.

Provencher, P. 2010. *Renforcement des dalles épaisses en cisaillement.* (M.Sc. Thesis) Université Laval, Québec, Canada.

Rahal, K. N., and Collins, M. P. 1999. Background to the General Method of Shear Design in the 1994 CSA-A23.3 Standard. *Canadian Journal of Civil Engineering*: **26**(6), 827-839.

Teng, J. G., Chen, G. M., Chen, J. F., Rosenboom, O. A., and Lam, L. 2009. Behavior of RC Beams Shear Strengthened With Bonded or Unbonded FRP Wraps. *Journal of Composites for Construction*: 394.

Valerio, P. 2009. *Realistic shear assessment and novel strengthening of existing concrete bridges.* (Ph.D. Thesis) University of Bath, Bath, United Kingdom.

Valerio, P., Ibell, T. J., and Darby, A. P. 2011. Shear Assessment of Prestressed Concrete Bridges. *Proceedings of the Institution of Civil Engineers - Bridge Engineering*: **164**(4), 195-210.

Villemure, F.-A., Fiset, M., Bastien, J., Mitchell, D., Fournier, B., and Bissonnette , B. 2016. Study of Bond Between Epoxy, Steel Reinforcing Bars and Concrete Affecter by Alkali-Silica Reaction. *15th International Conference on Alkali-Aggregate Reaction*, São Paulo, Brazil, 1:

Yoon, Y. S., Cook, W. D., and Mitchell, D. 1996. Minimum Shear Reinforcement in Normal, Medium, and High-Strength Concrete Beams. *ACI Structural Journal*: **93**(5), 576-584.